PAPER • OPEN ACCESS

Influence of carbon on energetics, electronic structure, and mechanical properties of TiAl alloys

New Journal of Physics
The open access journal at the forefront of physics

Deutsche Physikalische Gesellschaft DPG
IOP Institute of Physics

Published in partnership with: Deutsche Physikalische Gesellschaft and the Institute of Physics

OPEN ACCESS

RECEIVED
17 February 2021

REVISED
24 May 2021

ACCEPTED FOR PUBLICATION
18 June 2021

PUBLISHED
29 July 2021

PAPER

Influence of carbon on energetics, electronic structure, and mechanical properties of TiAl alloys

Dominik Legut[1,4,*], **Jürgen Spitaler**[2], **Pasquale Pavone**[3,4] **and Claudia Draxl**[3,4]

[1] IT4Innovations, VSB-Technical University of Ostrava, 17.listopadu 2172/15, CZ 70800 Ostrava-Poruba, Czech Republic
[2] Materials Center Leoben Forschung GmbH, Leoben, Austria
[3] Physics Department and IRIS Adlershof, Humboldt-Universität zu Berlin, Germany
[4] Previous affiliation: Chair of Atomistic Modelling and Design of Materials, Montanuniversität Leoben, Austria
[*] Author to whom any correspondence should be addressed.

E-mail: dominik.legut@vsb.cz

Keywords: mechanical properties, solubility, insterstitials, *ab initio* calculations

Abstract

We present first-principles calculations of carbon-doped TiAl alloys. The effect of carbon on the structural, electronic, and elastic behavior of the γ phase ($L1_0$ structure) of TiAl is investigated. The calculated enthalpy of formation at zero temperature indicates that carbon atoms favor to occupy rather interstitial than substitutional positions. The computed solubility of carbon in the stoichiometric γ phase is very low, in agreement with experimental findings. However, it is significantly enhanced for the Ti-rich alloy and when located inside Ti_6 octahedra. Mechanical properties such as Cauchy pressure, elastic anisotropy, Young's modulus, as well as Pugh and Poisson ratios of stoichiometric and off-stoichiometric compositions are analyzed as a function of carbon concentration and its location. As a general trend, we obtain that below a concentration of 3 at.%, carbon plays a minor role in changing the ductile behavior of γ-TiAl. A slight increase in ductility is found in the Ti-rich $\gamma\alpha$ phase if either located in the Ti-plane (Ti_4Al_2 octahedral site) or in a Ti_6 octahedra.

1. Introduction

TiAl alloys have been used in the last decades as structural materials at elevated temperatures, particularly for applications in gas turbines or in aerospace and automotive industries [1, 2]. They were intended to substitute conventional steels and Ni superalloys due to their attractive properties, such as very low density as well as high specific strength, stiffness, creep resistance, and oxidation resistance [1, 2]. The two main phases of TiAl are the tetragonal γ phase (labeled $L1_0$) and the hexagonal α_2 phase (labeled $D0_{19}$). Like many other intermetallic phases, γ-TiAl alloys suffer from poor ductility as well as low creep and oxidation resistance at temperatures above 1000 K. These shortcomings are even more pronounced for single-phase alloys based on the α_2 phase. Alloying this phase by Nb, Mo, and other transition elements, leads to increased ductility and strength. However, alloying by elements like Si—which is needed for increasing oxidation resistance—deteriorates many of the advantageous properties of TiAl alloys [3].

Two-phase α_2/γ-TiAl alloys exhibit much better mechanical properties than single-phase systems. The room-temperature ductility is sufficient, the toughness is increased, and the creep resistance is superior [4]. Unlike single-phase γ alloys, two-phase α_2/γ ones do not suffer from the anomalous temperature dependence of yield stress which is characteristic for intermetallic alloys [5]. The increase of ductility in two-phase systems could be related both to α_2/γ interfaces [1, 6] and to alloying elements, whose solubility can be much enhanced due to the lamellar structure of the α_2/γ phases [1].

Even though the industrial utilization of TiAl alloys relies on the lamellar α_2/γ structure, many theoretical and experimental investigations are dealing with single-phase γ or α_2 TiAl for better understanding their behavior. Among these studies, we quote the investigation of solutes partitioning into γ and α_2 phases [7], changes of c/a ratio and elastic properties with alloying by transitional elements (e.g. Mo,

W, Zr) [8, 67, 68], elasticity under pressure [9], as well as oxidation resistance and protective coatings hardening [10–12]. Concerning the mechanical properties of single phases, theoretical studies addressed the effect of alloying on cleavage strength [13] and to the stress–strain behavior [14, 15]. All above studies were related to the pure single phases or single phases alloyed by transition elements, their stability summarized in reference [74] and references therein.

It is commonly believed that alloying by substitutional elements may decrease the anisotropy of the electron distribution and, hence, increase the ductility of the alloy at room temperature [3]. A similar effect might be achieved by alloying the single phases (γ or α_2) with interstitials like B, C, O, and N. Several studies show a beneficial role of carbon additions in TiAl for mechanical properties at room and elevated temperatures [20, 71–73]. Available experiments give no clear answer to how large the solubility of C in the single phases is. Indeed, some experimental studies report an extremely low solubility of C and O, amounting to 150 and 260 ppm, respectively [16–18]. On the other hand, results of other investigations showed a C content in γ-TiAl up to 1 at.% [19], and even a carbon concentration as high as 2 at.% [20]. Recently in off-stoichiometric Ti–Al–Ta, a solubility of N up to 0.45 at.% was detected, while further increase of the N-concentration (up to 2 at.%) led to formation of Ti_2AlN [69].

In carbon-doped TiAl alloys, a crucial role seems to be played by the appearance of the hexagonal Ti_2AlC structure (often referred to as H-phase), which acts as a limiting factor for the solubility. Nevertheless, it is still unclear why the solubility of interstitials is higher in α_2 TiAl than in the γ phase [18]. A possible explanation is provided by the occupation of octahedral cavities by interstitial elements. Indeed, in carbides and nitrides, C and N atoms are surrounded by six Ti atoms [21]. Similar situations can be found in the $D0_{19}$ structure of the α_2 phase, where octahedral sites with a Ti_6-like and Al_2Ti_4-like configurations of the nearest neighbors are present. However, in the γ phase, where the coordination of Ti atoms is lower, only the Al_2Ti_4-like and Ti_4Al_2-like octahedral sites are formed.

There is a number of *ab initio* investigations dealing with carbon-doped TiAl systems, i.e., electronic-structure calculations of TiAl with substitutional and interstitial C [22]. However, neither the energetics of carbon in different octahedral configurations nor the effect of C on elastic properties has been quantitatively determined. A number of studies deal with carbon as a main constituent of P- and H-perovskite precipitate phases, investigating structure, electronic structure, bulk moduli, elastic constants, and cohesive energies [24–27].

In this work, we address several questions dealing with the role of carbon in γ-TiAl: why is the solubility of carbon so low? What is the preferred location of C? Can carbon in concentrations as low as the *real* ones still affect elastic properties? What is the role of local disorder on heat of formation and the elastic behavior?

The paper is organized as follows. In section 2 we describe the used methodology. Section 3.1 is devoted to the study of structural changes of γ-TiAl with interstitial C, and the effect of these changes on its electronic structure, elastic behavior, and mechanical properties. Section 3.2 deals with the structural and elastic properties of substitutional carbon, while section 3.3 presents results for a variant of the γ phase containing Ti_6 octahedra. Section 3.4 deals with the energetics of all considered structures, and concluding remarks are drawn in section 4.

2. Methodology

All *ab initio* calculations presented in this work have been performed within density-functional theory (DFT) using the projected augmented wave (PAW) method as implemented in the Vienna *ab initio* simulation package (VASP) [28]. The gradient corrected exchange–correlation functional parametrized by Perdew–Burke–Ernzerhof [29] was employed. A plane wave cutoff of 480 eV was used for most properties including geometry optimization, whereas for the calculation of the stress tensor the cutoff needed to be increased up to 1200 eV. Atoms were represented by PAW pseudopotentials provided by VASP with the $3p^6 4s^2 3d^2$, $3s^2 2p^1$, and $2s^2 2p^2$ valence electronic configuration for Ti, Al, and C atoms, respectively.

The Brillouin zone was sampled using Γ-centered Monkhorst–Pack grids of the following (almost) equivalent sets of points for different supercell sizes: a 20 ×20× 20 **k**-point mesh for the tetragonal TiAl unit cell with 4 atoms, a 30 ×30× 6 mesh for the hexagonal phase of Ti_2AlC with 8 atoms in the unit cell, and a 28 ×28× 13 mesh for the rhombohedral Al_4C_3 supercell with 21 atoms (in hexagonal settings). The partial occupancies were determined using the Methfessel–Paxton method [30] using a smearing width of 0.1 eV. A combination of conjugate-gradient energy minimization and a quasi-Newton force minimization was employed to optimize the geometry and atomic positions of the supercells. Atomic positions were relaxed until the forces were smaller than 10^{-4} eV Å^{-1}; total energies were converged within 10^{-6} eV.

In order to test the reliability of the chosen parameters, calculations were performed for pure γ-TiAl using supercells of different sizes. Deviations in the total energy for the optimized configurations were less than 0.4 meV atom^{-1}. Fitting the third-order Birch–Murnaghan equation of state [41] to the

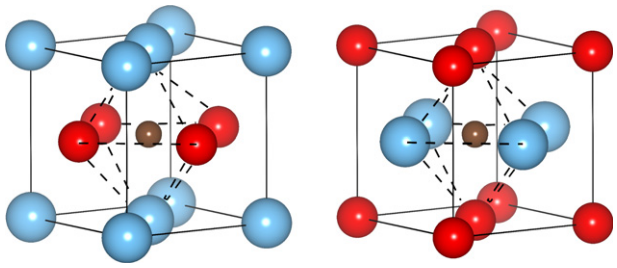

Figure 1. The two octahedral interstitial positions of carbon in γ-TiAl. Spheres with increasing radius denote C (brown), Al (red), and Ti (blue) atoms, respectively. The carbon atoms are located in a horizontal plane occupied only by either Al (left panel) or Ti (right panel) atoms, forming Al_4Ti_2 ($\gamma + C_{Al}$) or Ti_4Al_2 ($\gamma + C_{Ti}$) octahedra, with their nearest-neighbor atoms, respectively.

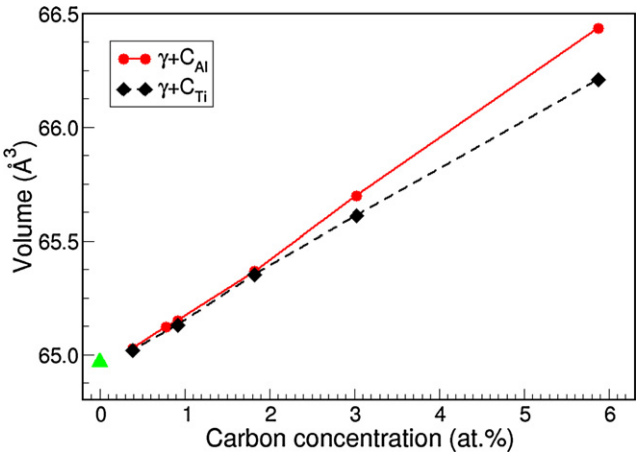

Figure 2. Unit cell volume V, in units of Å^3, of the γ phase containing two formula units, as a function of carbon concentration. Solid red and dashed black lines show the results for the system with a C atom located in the Al and Ti plane, respectively. For comparison, the volume of pure TiAl is indicated by the (green) diamond.

energy–volume curves for a four-atom-basis γ-TiAl with optimized c/a ratio, we obtained the lattice constants $a = 3.993$ Å and $c/a = 1.020$. Very similar values were calculated by fully optimizing supercells containing 16, 32, 54, 108, 128, and 256 atoms. The maximum deviation in the total energy was less than 0.75 meV per formula unit (f.u.) for the largest supercell (256 atoms). We note that at the investigated concentrations, the C–C distances in the Cartesian directions are unequal. However, this does not affect our results, as the valence charge density at the unit-cell boundary differs by less than 10^{-4}e from its counterpart in the pristine material. Overall, the calculated values of a and c are in very good agreement with both experiments ($a = 3.976$ to 4.00 Å and $c/a = 1.016$ to 1.023) [32–34] and previous first-principles studies ($a = 3.901$ to 3.96 Å and $c/a = 1.01$ to 1.037), calculated by pseudopotential [35, 36] and all-electron [37] methods, respectively.

3. Results and discussion

3.1. Interstitial carbon in the γ phase

3.1.1. Structural effects

The two possible octahedral positions of interstitial carbon in γ-TiAl are depicted in figure 1. In the first case (left panel), the C atom is located in the Al plane. The surrounding octahedron is formed by 4 Al and 2 Ti atoms. This configuration will be denoted in the following as $\gamma + C_{Al}$. In the second case (right panel), the C atom is situated in the Ti plane ($\gamma + C_{Ti}$), and the octahedron is formed by 4 Ti and 2 Al atoms.

The influence of C on the lattice was studied by fully relaxing the unit cell for different C concentrations and C located on both possible interstitial sites. It turned out that the tetragonal symmetry of the unit cell is preserved upon addition of carbon, and no distortion of the lattice vectors occurred. As shown in figure 2, the volume change as a function of the carbon concentration exhibits a linear behavior (Retger's law) [75] if the concentration is less than 6 at.%.

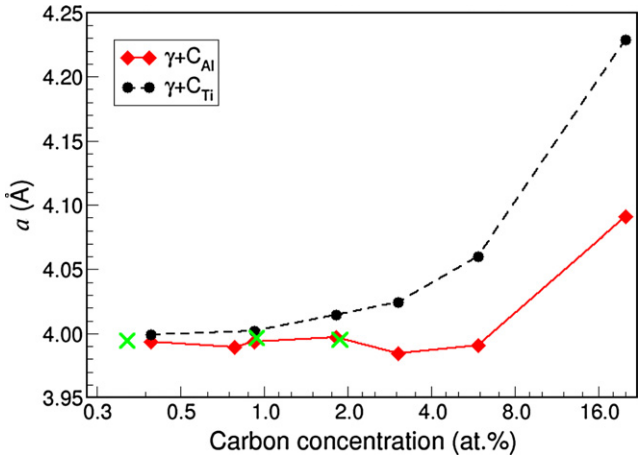

Figure 3. Lattice constant a, in units of Å, of γ-TiAl as a function of carbon concentration, for C located in the Al plane (solid line) and Ti plane (dashed line), respectively. The green crosses indicate experimental values from reference [20]. Note the logarithmic scale of the x-axis.

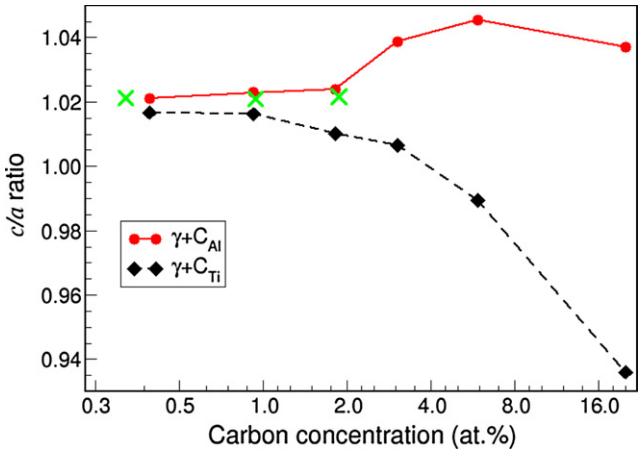

Figure 4. c/a ratio of γ-TiAl as a function of carbon concentration, for C located in the Al plane (solid line) and Ti plane (dashed line), respectively. The green crosses indicate experimental values from reference [20]. Note the logarithmic scale of the x-axis.

Trends of the lattice parameters a and c/a as a function of carbon concentration are shown in figures 3 and 4, respectively. Obviously, at both interstitial positions, the lattice constant a of the pure γ phase is approached with decreasing concentration of C. However, different behavior is found for the two kinds of octahedral sites. As seen in figure 3, for carbon within the Al plane ($\gamma + C_{Al}$), the lattice constant a is very similar to that of the pure γ phase for a range of concentrations up to about 6 at.%. In contrast, the presence of a C impurity in the Ti plane ($\gamma + C_{Al}$) expands the lattice constant a to a significant extent starting from 2 at.%. The variation of c/a as a function of carbon concentration is shown in figure 4. For the $\gamma + C_{Ti}$ case, the expansion of a is accompanied by a reduction of c/a. In contrast in the case of C in the Al plane, the c/a increases considerable in the range from 2–6 at.% of C, while getting slighlty smaller for 20 at.%.

A corresponding experimental study of carbon-doped TiAl has been reported in reference [20]. This work, however, refers to the non-stoichiometric alloy $Ti_{0.52}Al_{0.48}$ with a lamellar structure of both γ and α_2 phases. For the sake of comparison, these results (indicated by crosses) are also depicted in figures 3 and 4. Apparently, the experimental data are closer to our results for C in the Al plane (solid line) than to the ones for C in the Ti plane (dashed line).

3.1.2. Electronic properties

In order to characterize the electronic structure of γ-TiAl with C in both interstitial positions, we analyze the total densities of states (DOS) as well as the charge-density distribution in the crystal planes containing carbon atoms. In figure 5, the total DOS is plotted for C concentrations of 20 at.% (upper panel) and 0.9

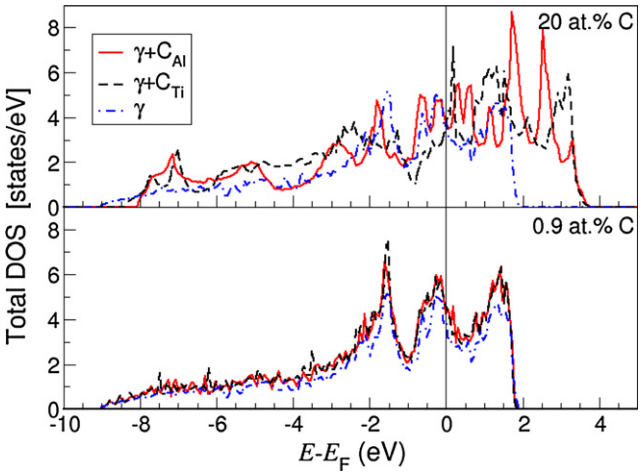

Figure 5. Total density of states of γ-TiAl for two C concentrations, with the interstitial carbon in the Al plane (solid line) and the Ti plane (dashed line), respectively. For comparison, the DOS of the pure γ phase is shown (dash-dotted line). The Fermi level is set to zero and denoted by a vertical line. The DOS in both panels is normalized to 2 formula units.

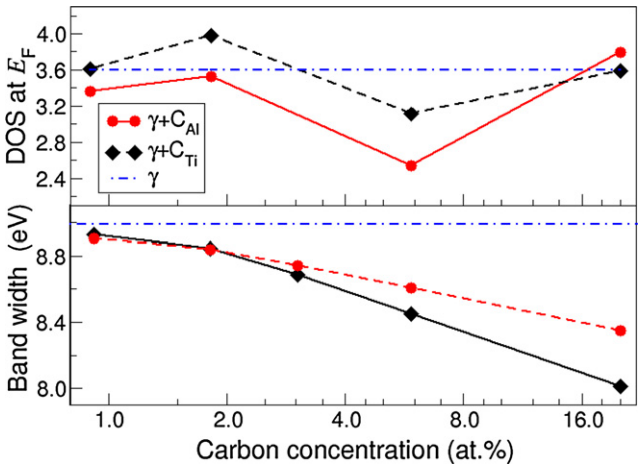

Figure 6. Total DOS at the Fermi level (in states per eV, normalized to two formula units; upper panel) and valence-band width (in eV; lower panel) as a function of C concentration, with the interstitial carbon in the Ti plane (solid line) and Al plane (dashed line), respectively. Note the logarithmic scale of the x-axis. The dash-dotted line corresponds to pure γ-TiAl and serves as a reference.

at.% (lower panel). For comparison, the total DOS of pure γ-TiAl is indicated by a dot-dashed line in both panels. The total DOS of the γ phase with 20 at.% C resembles the results of Matarand co-workers [22], which were obtained by the linear muffin-tin orbital method. For the higher carbon concentration, the DOS in the vicinity of the Fermi level is more affected, i.e. stronger hybridization occurs between C and Ti/Al atoms.

In figure 6, the DOS at the Fermi level (upper panel) and the valence-band width are shown as a function of carbon content (lower panel). Below 1%, both quantities are practically the same as those of the pure γ phase (see also lower panel of figure 5). The DOS at E_F oscillates around that of the pure γ phase, approaching it at low C concentrations. For high carbon content, the width of the top occupied band is less affected when carbon is in the Al-plane. This supports previous results that the more directional and stronger bonding occurs among carbon and Ti-atoms (Ti_4Al_2 octahedra) and is manifested by narrowing the top valence band.

To analyze the influence of carbon further, the difference in charge density between the cells with (ρ_{TiAl+C}) and without carbon (ρ_{TiAl}), $\Delta\rho = \rho_{TiAl+C} - \rho_{TiAl}$, is depicted in figure 7 for 20 at.% carbon being either located in the Al plane or Ti plane. Let us first consider the (100) plane (figure 7, left side): In the case of of C in the Al plane (upper panel), a filling of the the d_{z^2} orbitals (not shown) of the Ti atoms in the corner, pointing along z, is encountered, together with a pronounced charge accumulation between the Ti atoms along z (left and right edges of the plot). Both features clearly indicate a strengthening of the bonds

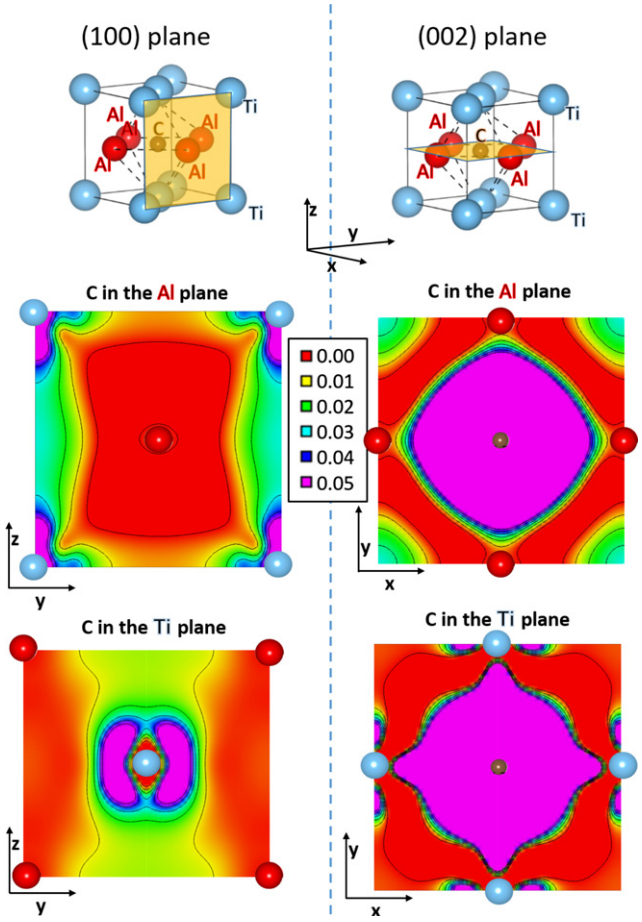

Figure 7. Contour plots of the difference in charge densities (in units of e Å^{-3}) between TiAl with and without C in the (100) plane (left side) and (002) plane (right side) for a carbon concentration of 20 at.%. The upper (lower) panels represent the structure with C in the Al (Ti) plane. The plots were done with XCrySDen [78].

in z direction. Considering the region between Ti atoms along y (top and bottom edge), only a small increase is seen. Interestingly, the Al atom in the center, which is the nearest neighbor of carbon, is not affected at all by its presence. The picture is completely different for C in the Ti plane (lower panel): a kidney-shaped charge accumulation around the Ti atom in the center is found, indicating that its $d_{x^2-y^2}$ orbitals (not shown) are getting filled. This goes along with a general increase in charge density above and below the Ti atom along the z direction. No increase in charge density is found between the Al atoms along z (left and right edge of the left figure). In contrast, the charge density between Al atoms along y increases (top and bottom edge), indicating a stiffening of the bonds in this direction.

Let us now turn to the (002) plane, i.e., the one where the C atom is located (figure 7, right side). First of all, in contrast to the case where C is in the Al plane (upper panel), for C in the Ti plane (lower panel) the change in charge distribution is rather asymmetric. In fact, it shows a spike pointing from C to the Ti atoms, manifesting the formation of Ti–C bonds. Second, for C in the Ti plane, a dumbbell shaped increase of charge density along the edges of the plot is seen, which indicates a filling of the $d_{x^2-y^2}$ orbitals. Conversely, the region around the Al atoms (upper panel), does not show any increase in charge density. This means, that the bonding in x direction is enhanced by C in the Ti plane, but is hardly affected by carbon in the Al plane.

3.1.3. Elastic behavior

In this section, the influence of interstitial carbon on the elastic constants is analyzed and discussed. The elastic constants are derived from stress–strain relations using the methodology by Yu *et al* [39] In order to get reliable results, both negative and positive distortions are considered. For high carbon concentrations in the pure gamma phase, we compare the elastic constants obtained from stress–strain relations to the ones derived from the second derivative of the total energy [48–50]. Both approaches lead to very similar results, differing by less than 2% for the single elastic constants.

Table 1. Elastic constants, C_{ij}, and bulk modulus, B, in GPa of the pure γ phase and with 3.03, 5.88, and 20 at.% interstitial carbon, either in the Al plane ($C_{Al-plane}$) or in the Ti plane ($C_{Ti-plane}$). They are obtained for the fully-optimized unit cell (opt). Experimental values are taken from reference [40].

	at.% C	C_{11}	C_{12}	C_{13}	C_{33}	C_{44}	C_{66}	B
Experiment	0.0	183	74	74	178	105	78	113
Theory, $C_{Al-plane}$	0.0	174	90	81	174	111	69	113
	3.0	176	85	80	187	105	69	114
	5.9	172	81	76	205	97	45	114
	20.0	171	124	70	309	44	34	129
Theory, $C_{Ti-plane}$	0.0	174	90	81	174	111	69	113
	3.0	172	91	86	172	106	64	116
	5.9	206	73	80	186	105	54	118
	20.0	294	68	65	265	87	63	143

The insertion of interstitial elements typically affects lattice parameters and chemical bonds in the host material, and, as a consequence, also the mechanical properties. The elastic constants as a function of C concentration, together with experimental results [40] for pure γ-TiAl, are summarized in table 1.

The pure γ phase of TiAl is overall well described by our calculations. Significant deviations from experiment are only found for C_{12} and C_{66}, amounting to about 20%. Similar differences were encountered in another theoretical work [9]. The bulk modulus can either be obtained as a function of total energy vs volume or using the elastic constants according to $B = (2C_{11} + 2C_{12} + 4C_{13} + C_{33})/9$ [48]. The values obtained with the two approaches differ by about 1 GPa only. The bulk modulus increases with C content for the phases with an interstitial C atom, suggesting an increase of the bonding strength. This effect is more pronounced for carbon positioned within the Ti plane, since here the C 2*p* states can more easily hybridize with Ti 3*d* states.

In the following, we examine in more detail table 1. If not mentioned explicitly, we always refer to the case of the optimized structure. Let us first consider the results for 20 at.%C, where a few observations can be made:

(a) C_{11} is strongly increased by carbon in the Ti plane, while C_{12} is slightly decreased.

(b) The presence of C in the Al plane does not affect C_{11}. We assign this behavior to the strong Ti–Al bonding (Al_4Ti_2 octahedra) that is not altered by C lying in the Al plane.

(c) C_{33} gets much stiffer upon adding carbon, where it has stronger impact in the Al plane than in the Ti plane. In the former case, C interstitials interact with the Ti atoms in adjacent layers above and below, forming a Ti–C bond along the *z* direction, as already shown in figure 7.

(d) C_{44} and C_{66} are clearly lower than in the pure γ phase, and they are twice as large in the case of C positioned in the Ti plane compared to the case of C in the Al plane. This behavior corresponds to the directional bonding between Ti and C, as it was already proposed in a number of publications [9, 14, 15, 23, 42].

Let us focus now on the results for lower carbon concentrations. There are two major trends (the same ones as in the γ phase):

(a) Carbon concentrations below 3% do not alter significantly the elastic constants of the γ-phase. At 3 at.%, the only increased values are found for the shear resistance, i.e., C_{12} for $\gamma + C_{Ti}$ and C_{13} for $\gamma + C_{Al}$.

(b) C_{ii} is high along the direction of C–Ti atoms, i.e. C_{11} for $\gamma + C_{Ti}$ and C_{33} for $\gamma + C_{Al}$, respectively. These values naturally decrease with lower carbon concentration. So, the decisive bonding here is the hybridization between carbon and titanium atoms which, at higher C concentrations, alters the bond strength and hence mechanical properties.

At a carbon content of 5.88%, C_{66}—the elastic constant associated with the shear between carbon-containing and carbon-free planes—shows a strong decrease for carbon located at both positions. At a content of 3.03 at.%, C_{11}, C_{44}, and C_{66} show almost negligible differences to the corresponding values of the pure γ phase. Also C_{11} and C_{33} are unaffected when C is located in the Ti plane.

Let us finally also compare our bulk moduli of the γ phase with C interstitials with those where carbon atoms form a carbide or a stable precipitate in the Ti–Al system. Going from the highest to the lowest value for B one finds: 270 GPa for TiC [27], 185 GPa for Ti_3AlC [24], 169 GPa for Ti_2AlC [27], and 130 GPa for Al_4C_3 [43]. It appears that a high bulk modulus is related to a high content of Ti atoms within the structure,

Table 2. Bulk modulus, B_C, calculated from single elastic constants [48], mechanical stability conditions (S_1, S_2, and S_3), and elastic anisotropy ratios (A_1, A_2, and A_3). Experimental values for pure γ-TiAl are taken from reference [40].

	at.% C	B_C	S_1	S_2	S_3	A_1	A_2	A_3
Experiment	0.0	110	212	990	181	1.43	1.98	1.35
Theory, $C_{Al-plane}$	0.0	114	186	1026	186	1.64	2.40	1.61
	3.0	114	203	1029	180	1.52	2.07	1.52
	5.9	113	225	1015	183	0.99	1.72	2.16
	20.00	131	340	1179	217	1.45	0.51	1.27
Theory, $C_{Ti-plane}$	0.0	114	186	1026	186	1.64	2.40	1.61
	3.0	116	172	1042	172	1.58	2.47	1.66
	5.9	118	232	1064	199	0.81	1.81	1.94
	20.0	139	429	1249	284	0.56	0.81	1.38

as already found in reference [27]. From our results, we find a simple relation: the bulk modulus of phases where carbon is located at interstitial positions is lower than in the case where carbon leads to the formation of intermetallic compounds where it is more strongly bound.

3.1.4. Mechanical stability and ductility

Based on the calculated elastic constants and the analysis of the charge-density, we predict a change of the mechanical stability and ductility (brittleness) of γ-TiAl upon carbon doping. In order to be stable against any homogeneous elastic deformation, a crystalline material has to fulfill stability conditions with respect to its symmetry [51]. Considering tetragonal systems, the elastic constants C_{11}, C_{33}, C_{44}, and C_{66} must be positive, and $C_{11} > C_{12}$. Such criteria are satisfied by both the pure and C-alloyed γ-TiAl phases as is evident from table 1. More restrictive conditions suggested by Beckstein and co-workers [49] are the following:

$$\begin{aligned} S_1 &= C_{11} + C_{33} - 2C_{13} &&> 0 \\ S_2 &= 2C_{11} + C_{33} + 2C_{12} + 4C_{13} &&> 0 \\ S_3 &= (2C_{11} + C_{33})/3 &&> B \end{aligned}$$

.As can be seen in table 2, all three stability conditions are fulfilled for both interstitial sites of C, for any concentration considered here (20 at.%, 5.88 at.%, and 3.03 at.% C). Indeed, the corresponding values are in most cases even higher than those for pure γ-TiAl, and they increase with carbon concentration.

The elastic anisotropy [52] tells us about the system's shear resistance, i.e., the energy change in a crystal associated with the shear modes along different slip directions. There are three elastic anisotropy ratios in tetragonal systems, defined as:

$$\begin{aligned} A_1 &= 2C_{66}/(C_{11} - C_{12}) \\ A_2 &= 4C_{44}/(C_{11} + C_{33} - 2C_{13}) \\ A_3 &= C_{44}/C_{66}. \end{aligned}$$

The denominator in the anisotropy coefficient A_1 represents a tetragonal shear (e.g. in (001) plane or equivalent), while A_2 corresponds to a shear along [011] in the $(0\bar{1}1)$ plane [55]. C_{66} and C_{44} correspond to the shear resistance along [010] and [100] in the (001) and (010) plane, respectively [55–57]. The location of carbon modifies the elastic anisotropic ratios with respect to the pristine material (see table 2). The difference between its calculated and experimental elastic constants defines the error range. Despite this uncertainty [79], a clear trend toward lower elastic anisotropy ratios A_1 and A_2 of the carbon rich material is observed, with the values for higher C concentrations (20 at.% and 5.88 at.%) being smaller by a factor of 2–3. At 3.03 at.% C, A_1 is slightly lower than the one of the pure γ phase, and A_2 and A_3 are also very close in $\gamma + C_{Al}$. However, for the carbon in the Al-plane, the A_2, and A_3 still differ from those of the pristine phase, see table 2). This stems from the enhanced stiffnes by bonding among the carbon and Ti atoms along the z-direction. Indeed, the anisotropy coefficient A_3, representing the shear of intra-layer and inter-layer bonds, is the one being most affected via C_{44}. One may conclude that about 3 at.% is the decisive concentration where carbon atoms still can modify the interlayer bonding as reflected by the decrease of the C_{44} of about 5%. Any lower concentration will not have any impact.

Based on the single-phase elastic constants we investigate a change of the B/G ratio or its inverse (G/B), respectively, upon carbon alloying. These two quantities are, at least qualitatively, a measure for the ductility

Table 3. Cauchy pressures (C_1 and C_2), Hill's averaged ratio (B/G), elastic anisotropy (A), Poisson ratio (ν), and Young modulus (E) for polycrystalline carbon-alloyed γ-TiAl. C_1, C_2, and E are given in GPa.

	at.% C	C_1	C_2	B/G	A	ν	E
Experiment	0.0	−3.9	−31	1.84	0.325	0.270	156
Theory, $C_{Al-plane}$	0.0	21	−30	2.07	0.387	0.292	141
	3.0	16	−25	2.06	0.358	0.291	132
	5.9	26	−24	2.00	0.276	0.286	149
	20.0	5	−22	3.7	0.439	0.376	96
Theory, $C_{Ti-plane}$	0.0	21	−30	2.07	0.387	0.292	141
	3.0	28	−20	2.23	0.385	0.305	136
	5.9	19	−25	1.96	0.282	0.282	154
	20.0	90	26	1.84	0.208	0.270	19

and the degree of covalency, i.e., directionality of bonding. Similarly, the ductile behavior was proposed to be related to the so-called Cauchy pressures [58]. Even though the Cauchy relations were questioned [56], they are still widely used a material's ductility. For tetragonal systems, the Cauchy pressures are defined as:

$$C_1 = C_{12} - C_{66}$$

$$C_2 = C_{13} - C_{44}$$

.Positive or negative values of C_1 and C_2 indicate ductile or brittle behavior, respectively. Measured elastic constants suggest brittle behavior of the γ phase at room temperature (see table 3). In contrast to this, but in agreement with other calculations [9, 37], we find C_1 positive ($T = 0$ K results). Note that experimentally reported values for C_{66} and C_{44} show a significant spread, see reference [34] and references therein. For C concentrations lower than 6 at.% C_1 is always positive, whereas C_2 is always negative, but less than in the pristine γ phase (see table 3). For the C-alloyed γ phases the values of C_2 are less negative than those of pure γ-TiAl. Suprisingly, carbon contributes to a higher DOS in the vicinity of the Fermi level, thus increasing metallicity. In other words, the presence of carbon increases the ductility (see table 3).

As an empirical rule found by Pugh [59], a B/G ratio of 1.75 separates ductile ($B/G > 1.75$) from brittle ($B/G < 1.75$) materials. The inverse ratio (G/B) indicates the relative degree of directional bonding, supposing that the bulk modulus corresponds to the average bond strength and the shear modulus to the resistance against changing the bond angles as discussed in reference [38]. For macroscopic samples, one should use average values of the different single crystal shear moduli, as the polycrystalline specimen, composed of differently oriented grains, is more isotropic. To mimic such polycrystalline materials, minimum and maximum values of the elastic constants are obtained by either imposing uniform strain (Voigt notation) or uniform stress (Reuss notation), see reference [52] and references therein. Therefore, we calculate the Voigt and Reuss bounds for shear (G_V, G_R) and bulk (B_V, G_R) moduli and obtain their averages (G_H, B_H) as proposed by Hill [60]. In the following, we always refer to the Reuss–Voigt–Hill averaged values of B_H, G_H, E_H, and A_H, and we define the elastic anisotropy ratio as

$$A_H = \frac{G_H - B_H}{G_H + B_H}.$$

For the averaged quantities we also drop the indices, e.g. $A_H \to A$, $B_H \to B$.

In table 3, we show B/G values for different carbon concentrations. Despite the fact that the experimental B/G value of the γ phase is slightly above 1.75, TiAl is known to be brittle at ambient conditions [1]. Our calculated results show that the γ phase with C located in the Ti-plane has a B/G ratio above the one of the pure γ phase, while for the material with C located in the Al-plane it is converse. For 3.03 at.% carbon content, the G/B ratios are similar to pure γ-TiAl if C is located in the Al-plane, but higher if C is in the Ti-plane, reflecting the higher degree of hybridization with the four neighboring Ti atoms and an increase of ductility [34]. The elastic anisotropy ratio A, with G and B as obtained by Hill's approximation [60], becomes lower as the C concentration is decreased. At 3.03 at.%, A is lower (higher) when C is in the Al-plane (Ti-plane). The last columns of table 3 summarize the results for the Poisson ratio, ν, and the Young modulus, E. The trends for the lowest C concentration are clearly independent of the carbon location. Lower values of E and G and higher ν correlate with weaker and less directional interatomic bonding, and hence with an increase of ductile behavior [62]. This is the case for interstitial C located in the Ti-plane.

The effect of carbon on the elastic constants can be compared to alloying by transition elements. In the work of Music and Schneider [8], it is shown that the bulk modulus and C_{44} are only slightly increased

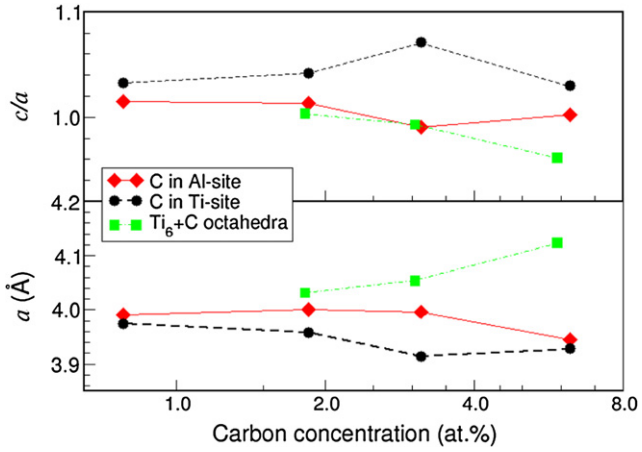

Figure 8. Change of lattice parameter a and c/a ratio as a function of carbon concentration for substitutional carbon. Solid red and dashed black line correspond to substitution of Al and Ti, respectively. The dash-dotted green line denotes the case of a Ti_6 octahedron surrounding the interstitial C. Note the logarithmic scale of the x-axis.

Table 4. Elastic constants of γ-TiAl with substitutional carbon (3.12 at.%) in the Al-plane ($\gamma + C_{Al}^{sub}$) and Ti-plane ($\gamma + C_{Ti}^{sub}$), respectively.

	C_{11}	C_{12}	C_{13}	C_{33}	C_{44}	C_{66}	B_C
Pure γ	183	74	74	178	105	78	113
$\gamma + C_{Al}^{sub}$	112	143	88	176	102	68	115
$\gamma + C_{Ti}^{sub}$	170	74	74	167	90	82	105

upon alloying TiAl with 6.25 at.% of 3*d*, 4*d*, and 5*d* metals, C_{44} going from 126 to 128 GPa. However, in this work, C_{44} of 126 GPa for the pure γ phase is rather high, i.e. about 20% higher than the experimental value of Tanaka *et al* [34] as well as our and other DFT results [9, 37]. Overall, we conclude that interstitial carbon has higher impact by significantly lowering C_{44} (see table 1) than alloying by transition metals.

Recently, Kanchana [24] reported results for B/G, E, and ν for perovskite Ti_3AlC [24], with values of 1.70, 272 GPa, and 0.255, respectively. Again, the conclusion can be drawn, that if the carbon atoms are constituents of the structure the material is more brittle than the γ phase with up to the 20 at.% of carbon atoms just located at any of the interstitial positions.

3.2. Substitutional C

There is a finite probability of C to occupy an Al or Ti site. The work of Matar and Etourneau [22] suggests that carbon prefers the Al site and stabilizes the TiAl-phase. In figure 8, we show how the calculated lattice constant a and the c/a ratio change upon C substitution on both sites. Again, it clearly illustrates the trend that C on an Al site does not interact strongly with the Ti and Al atoms. It slightly expands the lattice constant a and makes the structure almost cubic ($c/a \approx 1$). The much stronger influence is found for Ti substitution. Here, the lattice constant is smaller (the c/a ratio higher) than for the pristine phase as the carbon *sp* states strongly hybridize with neighboring Ti atoms. Therefore, the carbon concentration has to be far below 1 at.% to have no influence.

The effect of substitutional C on the elastic properties of TiAl are summarized in table 4. The values for Al-substitution do not seem to be reasonable at first glance as, for a system with almost cubic symmetry, it is expected that $C_{11} \approx C_{33}$, $C_{12} \approx C_{13}$, and $C_{44} \approx C_{66}$. The first two relations are, on the contrary, fulfilled for C at the Ti site. So, why is this so? The reason for the surprising elastic behavior of C at the Al-site is that the Ti atoms surrounding carbon in the first two adjacent layers are unevenly shifted from their original x (y) or z positions by 1.3% and 2.7% respectively. Already in the next layer these displacements are only 0.4% and 0.7%, respectively. In contrast to this, having carbon at the Ti-site, four Ti atoms in the first coordination shell are shifted in x and y direction simultaneously, preserving the tetragonal symmetry. Therefore, carbon at the Ti-site (3.12 at.%) leads to an almost cubic phase (lower a and $c/a \approx 1$) demonstrated by the elastic constants resembling the ones of a cubic system, except for the values of C_{44} and C_{66}.

Substitution of Al makes C_{12} and C_{13} stiffer but C_{11} and C_{44} softer. Therefore the stability criterion $C_{11} > C_{12}$ does not hold any more, and the compound becomes inherently unstable. Substituting Ti by carbon makes C_{33} and C_{44} softer, while C_{66} is getting much harder. Quantifying the most important changes

Table 5. Elastic constants, bulk moduli obtained from single elastic constants B_C, and Cauchy pressures (in GPa) as well as B/G, averaged elastic anisotropy factor A, Poisson ratio ν, and Young modulus E (in GPa) of the off-stoichiometric γ phase containing Ti octahedra without ($\gamma + Ti_6$) and with interstitial carbon ($\gamma + Ti_6 + C$). The example represents a Ti:Al ratio of 56:44 with a carbon concentration of 3.03 at.%. For comparison, the results of the pure γ phase are shown.

Phase	C_{11}	C_{12}	C_{13}	C_{33}	C_{44}	C_{66}
Pure γ	174	90	81	174	111	69
$\gamma + Ti_6$	169	81	80	162	103	49
$\gamma + Ti_6$+C	176	83	91	164	103	60

Phase	B_C	C_1	C_2	B/G	A	ν	E
Pure γ	114	21	−30	2.07	0.387	0.292	141
$\gamma + Ti_6$	112	32	−16	2.26	0.359	0.308	130
$\gamma + Ti_6 + C$	116	23	−12	2.25	0.352	0.306	135

induced by the substituents, the elastic anisotropy ratio A_3 for C at the Al-site is about 40% higher than that for C at the Ti-site. We conclude this section by stating that if carbon enters the γ phase substitutionally at the Ti site, it makes the material softer by lowering the bulk modulus and decreasing the shear modulus C_{44}. A substitution of carbon at the Al-site is very unlikely to be found, as the elastic constants point to an intrinsic instability of such solid.

3.3. Effect of Ti_6-octahedra formation

The first coordination shell of interstitial carbon in the regular γ phase is composed of 4 Ti and 2 Al atoms or vice versa, see figure 1. However, in the α_2-phase of Ti–Al alloys, the octahedral interstitial position is formed solely by 6 Ti atoms. Scheu and co-workers [31] suggested that also in the γ phase carbon would prefer a location of complete Ti_6 octahedra, i.e., octahedra where the Ti atoms also occupy the two Al sites, similarly to the α_2-phase. Moreover, they considered such arrangement to be responsible for a higher solubility of carbon in the α_2-phase. Therefore, we investigate the influence of such a 'local disorder' by calculating the corresponding elastic behavior and heat of formation. Already for moderate Ti-rich concentrations, the c/a ratio goes toward 1, without any effect from the carbon atom occupying an interstitial position in Ti_6 octahedra. This is in contrast to the situation where carbon substitutes the Ti- or Al-sites. The presence of carbon inside Ti_6 octahedra expands a only slightly, but to a larger extent than carbon substitution of Al or Ti (see figure 8). For concentrations less than 3 at.% the compound becomes cubic (see figure 8). The elastic constants of the γ phase containing Ti_6 octahedra are summarized in table 5. First, the C_{ij} wrt. to the ones of pure γ phase are softer, as the lattice expands (see lines 2 and 6 of table 1), second, by the presence of carbon (3.03 at.%) the initial elastic stiffness of the material is restored. In the precipitate compound Ti_3AlC the same Ti_6 octahedra surrounding carbon atoms exists. The elastic behavior of this phase was calculated by Kanchana [24], obtaining a C_{44} of 89 GPa. This is very close to our values of γ-TiAl with 20 at.% C located in the Ti-plane (see table 1); but it is by ca. 20% lower than those of the pure γ phase and the γ phase with Ti_6 octahedra and/or very low carbon concentration. Concomitantly, Ti_3AlC has a bulk modulus more than 50 GPa higher ($B = 185$ GPa) than that of the γ phase with 3.03 at.% of carbon or less (with or without Ti_6 octahedra). This indicates very interesting elastic behavior. The periodic occurence of the carbon atoms in the structure increases the resistance against hydrostatic pressure (bulk modulus), but at the same time lowers the shear resistance with respect to the pure γ phase.

The elastic constants as well as the bulk modulus of the γ phase with incorporated Ti_6 octahedra indicate that this material is somewhat softer than the pristine phase (see tables 5 and 1). Occupying Ti_6 octahedra by carbon slightly expands a, where one could expect a softening of C_{11} and C_{33}. However, our results show the opposite effect, i.e. a stiffer material with some values of C_{ij} being higher by about 7–10 GPa. These values are comparable to or only slightly larger than those of the γ phase with 3.03 at.% or less interstitial carbon, regardless of its location (see tables 5 and 1).

We conclude this section by stating that the formation of Ti_6 octahedra enhances the ductility of the γ phase to the same extent as carbon alloying. No further effects by carbon located in (off-stoichiometric) Ti_6 or Ti_4Al_2 octahedra on the ductility are found.

3.4. Energetic considerations and C site-preference

3.4.1. Substitutional and interstitial C in the regular γ phase

For considerations on the energetics, we adopt the approach of chemical potentials as described in references [53] and [54]. We obtain the chemical potentials of Ti and Al from the total energies of the pure

Table 6. Chemical potential of carbon, μ_C (in eV atom^{-1}), derived from a number of stable carbides by employing constant chemical potentials of Ti and Al, and lattice parameters (in Å).

Phase	μ_C	a_{calc}	a_{exp}	c_{calc}	c_{exp}
TiC	−10.695	4.338	4.32 [44]		
Ti_3AlC	−11.074	4.183	4.16 [45]		
Ti_2AlC	−11.075	3.069	3.058 [26]	13.742	13.642 [26]
Al_4C_3	−8.576	3.354	3.333 [46]	25.118	24.997 [46]
Diamond	−9.090	3.573	3.567 [76]		
Graphite	−9.221	2.458	2.464 [77]	7.831	6.711 [77]

γ TiAl and α_2 Ti_3Al phase, respectively, yielding $\mu_{Ti} = -8.102$ eV and $\mu_{Al} = -4.399$ eV, in accord with similar values as in reference [7]. The chemical potential of carbon, μ_C, will be treated as a variable. The stable carbides of pure Al and Ti are naturally Al_4C_3 and TiC. However, as indicated by many experiments [45, 64], aging and quenching of C-doped TiAl alloys at high temperatures (above 1000 K) yields a metastable cubic perovskite phase of Ti_3AlC and, after a longer time, a stable hexagonal phase of Ti_2AlC. Consequently, it would be these phases that are in equilibrium with the γ- and α_2-phases, and hence their chemical potentials should be the most relevant ones. Recently, electronic structure and mechanical properties of Ti_3AlC and Ti_2AlC were investigated from first-principles, and the phase stability of these precipitates was verified experimentally, see references [24–27].

Table 6 summarizes the experimental and calculated lattice parameters of TiC, Al_4C_3, Ti_2AlC, and Ti_3AlC, and the corresponding chemical potentials of carbon μ_C derived from the total energies of these stable carbides using constant values for μ_{Al} and μ_{Ti}. In order to facilitate the comparison of our results with literature data, using the chemical potentials of C derived from graphite or diamond [74], the corresponding data are also added.

In general, the thermodynamic free energy is temperature dependent. One contribution to this temperature dependence is the configurational entropy that lowers the enthalpy of formation (see equation (2) in reference [7]). Despite the fact that, at higher temperatures, the entropy term as well as the shift of chemical potentials play a role [7], for simplicity, both are omitted here. In figure 9, the enthalpy of formation is shown as a function of C concentration (as justified above the μ_C from the $TiAl_2C$ is used here), for both interstitial positions (upper panel) and C substituting Al and Ti (lower panel). Two models are considered: solid lines correspond to a model with fully optimized geometry after insertion of or substitution by a carbon atom, while dashed lines denote the situation where the lattice constant a and the c/a ratio are fixed to the values of the pure γ phase, and only the atomic positions are relaxed. From figure 9 it is apparent that the C atom prefers to incorporate itself into the γ phase as an interstitial rather than to substitute Al or Ti atoms, as the energy scale for the former is much lower than the one for the latter. A study by Matar am co-workers [22], based on the DOS and analysis of the crystal-overlap-population, did not give a decisive answer which position C would prefer. In contrast, figure 9 clearly shows for a large concentration range that the interstitial position in the Ti-plane of the γ phase is preferred by about 1.5 eV compared to interstitial carbon located in the Al-plane (upper panel). However, the energy cost of incorporating the carbon atom is indeed higher than the calculated antisite energies of stoichiometric TiAl of 0.7 eV and 0.3 eV for Ti and Al sites, values being in accord with other studies [7, 37].

A work of Liu *et al* [70] indicates that interstitial oxygen within γ-TiAl increases the impurity-formation energy. Interestingly, if carbon substitutes Ti at a C concentration lower than 4 at.%, H_f is higher than in the case where Al is replaced by C, as evident from figure 9. Let us point out one more aspect here: the enthalpies of formation for the above described models, denoted by solid and dashed lines in the upper panel of figure 9, start to coincide below a concentration of 2 at.%. In the same concentration range, very small variations of a and c/a are observed as indicated in figures 3 and 4. It also coincides with the a and c/a values for the highest carbon concentration found in the γ phase experimentally. This indicates that, reaching higher carbon concentrations in the Ti–Al system would go hand-in-hand with an increase in energy, which is an unlikely scenario. It seems that carbon located at the Ti or Al sites of the γ phase introduces so-called Friedel oscillations [47], i.e. oscillations of the charge density, as indicated by a somewhat oscillating behavior of a and c/a as well as H_f, see figures 8 and 9.

As evident from table 6, μ_C can vary over a certain range (−8.576 to −11.075 eV atom^{-1}). However, the highest value, derived from Al_4C_3, can be disregarded since it leads to a negative enthalpy of formation for any interstitial positions of C in the γ phase. As stated above, in many experimental studies of TiAl alloys (see, e.g., reference [22]), carbon is introduced via TiC, and due to high temperature, aging, or other treatments, the carbides Ti_3AlC and Ti_2AlC are formed. Therefore, these precipitates are in equilibrium with the γ-phase as well as with α_2-TiAl. This fact justifies to reduce μ_C to values bounded by TiC and

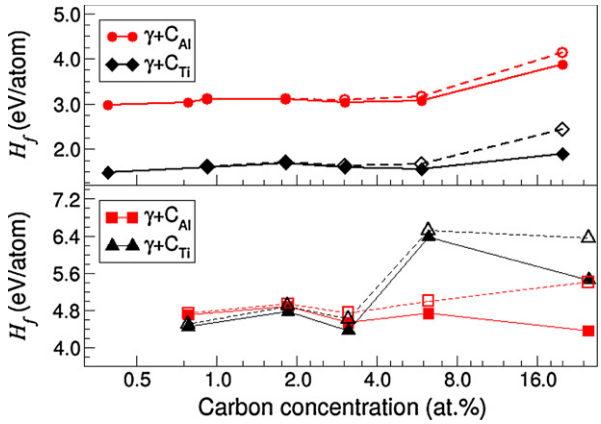

Figure 9. Enthalpy of formation (H_f) of γ-TiAl as a function of C concentration for the cases of interstitial carbon (upper pannel) and substitutional carbon (lower pannel). C located in the Al-plane (Ti-plane) is marked by a black (red) line. Solid lines denote full relaxation, dashed lines stand for relaxation of atomic positions only, with a and c/a fixed to the values of the pure γ phase. Note that the x axis is in logarithmic scale.

Ti_2AlC, i.e., to the range of -10.695 to -11.075 eV/atom. Employing different values for μ_C, one can lower or increase the enthalpy of formation and the corresponding equilibrium concentration of solute carbon, corresponding to different thermodynamic equilibria or experimental conditions of alloy formation. From table 6 it is apparent that the chemical potential of C obtained using Ti_2AlC and Ti_3AlC are very similar, in accord with previous calculations [7]. The processing temperature of TiAl alloys with TiC as a carbon reservoir is high, i.e., $T = 1623$ K [20], such that the configurational entropy—a negative term—would play a role and decrease the thermodynamic free energy [7].

The equilibrium solute concentration c(i) is related to the enthalpy of formation (neglecting the configurational entropy term) by the exponential expression [7, 53, 54]:

$$c(\mathrm{i}) = \exp\left(-\frac{H_\mathrm{f}}{k_\mathrm{B}T}\right), \tag{1}$$

where, for our situation, all quantities are already known. One reaches a converged enthalpy of formation by increasing the supercell or, equivalently, decreasing the concentration of atomic impurities. From figure 9 one can see that for both interstitial positions, H_f exhibits a plateau for carbon concentrations lower than 6 at.%, oscillating around the mean value by not more than 0.1 eV atom^{-1}. The energy difference related to the two different interstitial positions occupied by carbon is nearly constant, i.e, about 1.5 eV atom^{-1}.

Employing the chemical potential of TiC as upper bound and the one of Ti_2AlC as lower bound, then, for a temperature of $T = 1623$ K [20], the resulting concentration of interstitial carbon located in the Ti-plane is of the order of 180–2720 ppm, whereas it is negligible for the one in the Al-plane (0.005–0.07 ppm). These results are in good agreement with values found by atomic-probe analysis of single-as well as two-phase TiAl alloys [16, 18].

3.4.2. Effect of Ti_6 *octahedra on the enthalpy of formation*

The formation of a Ti_6 octahedron where the C atom is located in the Ti-plane involves substitution of two Al atoms by Ti (2 antisites). This leads to a non-stoichiometric (Ti-rich) alloy, which impacts the chemical potentials of Ti and Al. We follow the work of Woodward *et al* [37] to obtain the chemical potentials, μ_{Ti} and μ_{Al}, for the non-stoichiometric (Ti-rich, Al-rich) γ phase, which are related to the antisite energies depending on the defect concentration. From references [37] and [65] it follows that formation of a second antisite is at zero energy cost. The contributions to the enthalpy of formation concern (i) the formation of Ti_6 octahedra; (ii) C entering into γ-TiAl already containing Ti_6 octahedra; (iii) the combination of both. The chemical potential for carbon is here again the one taken from $TiAl_2C$.

Figure 10 shows H_f, incuding all three contributions, as a function of C or Ti concentration, using equation (1) and $T = 1623$ K as in figure 9. The result for forming Ti_6 octahedra is indicated by a dash-dotted green line, showing a decrease of energy as the system goes toward more Ti-rich concentrations, i.e., higher Ti_6 content (top x axis). Eventually, μ_{Ti} adopts the same value as for pure hcp Ti, i.e., lower in energy than the one for Ti in the γ phase. The opposite trend is visible for C entering γ-TiAl (red dashed line) as well as the overall trend, i.e., the probability of inserting Ti_6 octahedra occupied by carbon into the pure stoichiometric γ phase (black solid line). We conclude that the energy cost for low carbon concentrations entering Ti_6 octahedra is about two times lower than for carbon to be soluted into

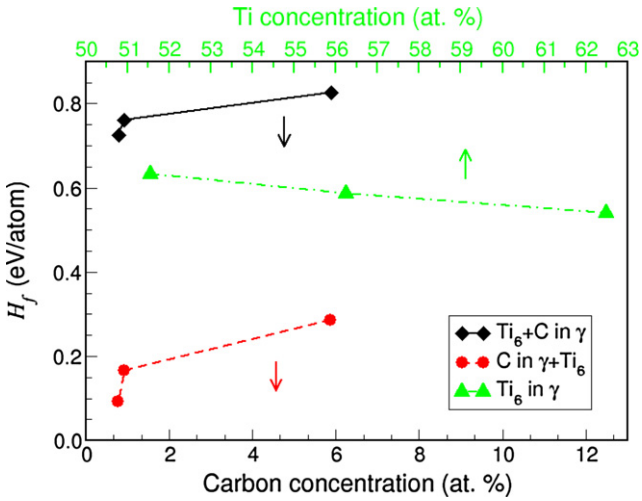

Figure 10. Enthalpy of formation (H_f) for creating Ti_6 octahedra occupied by carbon in stoichiometric γ-TiAl (solid black line), C in γ-TiAl already containing Ti_6 octahedra, i.e., Ti-rich (dashed red line), and Ti_6 octahedra with respect to stoichiometric γ-TiAl (dash-dotted green line, upper axis).

stoichiometric γ-TiAl, i.e., inside of Ti_4Al_2 or Ti_2Al_4 octahedra (compare black solid lines of figures 10 and 9 (upper panel)). If one uses $\mu_C(Ti_2AlC)$, then the corresponding solubility of carbon is about 0.2–0.5 at.%, i.e., definitively higher than for the stoichiometric γ phase, which is in very good agreement with experimental studies [19, 20].

4. Conclusions

Total-energy calculations have revealed that in the γ phase of TiAl, carbon atoms rather occupy interstitial than substitutional positions. An interstitial position in the Ti-plane is preferred over the Al-plane by ≈1.5 eV for any carbon concentration lower than 6 at.%. But even for C in the Ti-plane, the energy of formation (enthalpy of formation at $T = 0$ K) is about 1.2 eV, which is comparable to the one of a vacancy [7, 11, 37, 65]. As a consequence, the expected concentration of interstitial carbon is very low, i.e., in the range of 180–2720 ppm, in accord with experiment [16, 18]. Indeed, the energy cost to solute carbon within the γ phase is higher than the energy of formation of Ti and Al antisites in stoichiometric TiAl, which is ≈0.7 eV and 0.3 eV, respectively, in accord with literature [7, 37]. For off-stoichiometric Ti-rich γ-TiAl, however, where Ti_6 octahedral positions are occupied, the solubility of carbon is much higher (by at least a factor two), and the probability of carbon to sit on an interstitial position inside such an octahedron is higher than on corresponding interstitial sites in stoichiometric TiAl. Since in experiment, an expansion of both a and c/a is observed, we suggest that a mixture of both interstitial sites is present in C-alloyed γ-TiAl, with a higher probability of carbon to be found in the Ti-plane.

The bonding properties and electronic structure of γ-TiAl are not significantly affected by carbon concentrations lower than about 1 at.%. At such a concentrations, the Fermi level and the DOS at the Fermi energy are similar for γ-TiAl with or without C interstitial. An analysis of the change in charge density due to carbon addition for the largest C concentration reveals that C partially fills the Ti d orbitals, but affects the bonding of Al rather little. For the case of C in the Ti plane, the bonds in the (x, y) plane are strengthened. For C in the Al plane, a very pronounced enhancement of the Ti–Ti bonds along z is found.

If carbon occupies one of the interstitial octahedral or substitutional sites, it affects the lattice constants and also the mechanical properties, depending on the concentration. We predict the elastic behavior of γ-TiAl including substitutional or interstitial C as well as of the Ti-rich material. Elastic anisotropy, Cauchy pressures, Pugh ratio, Poisson ratio, and Young modulus have been computed to quantify the effect of C on the ductility of γ-TiAl as a function of C concentration. These criteria reveal, for example, that C alloying at a concentration of about 3 at.% increases the ductility only very slightly, owing mainly to the position of C in the Ti-plane. At a similar concentration, substitutional C affects the elastic properties to a larger extent. In contrast, for the case of C located at the Al-site, the elastic constants indicate that such a solid is intrinsically unstable.

For C concentrations lower than 3 at.%, which correspond to the concentrations of the experimentally characterized samples reported in literature, we conclude that the mechanism of ductilization is not related to the presence of interstitial C within the bulk γ phase. It will be interesting to shed further light on

whether a possible mechanism of ductilization is promoted by segregated carbon at grain boundaries or α_2/γ interfaces in the lamellar structure of the material. We anticipate that the role of interstitial carbon (and possibly other interstitials) must be more pronounced at grain boundaries, interfaces, and extended defects than within bulk γ-TiAl.

Acknowledgments

We gratefully acknowledge financial support under the scope of the COMET program within the K2 Center 'Integrated Computational Material, Process and Product Engineering (IC-MPPE)' (Project No. 859480). This program is supported by the Austrian Federal Ministries for Climate Action, Environment, Energy, Mobility, Innovation and Technology (BMK) and for Digital and Economic Affairs (BMDW), represented by the Austrian research funding association (FFG), and the federal states of Styria, Upper Austria and Tyrol. DL acknowledges support by the ERDF in the IT4Innovations national supercomputing center-path to exascale Project (CZ.02.1.01/0.0/0.0/16_013/0001791) within the OPRDE and and the Project e-INFRA CZ (ID:90140) by the Ministry of Education, Youth and Sports of the Czech Republic and by Czech Science Foundation Project No. 20-18392S. JS acknowledges financial support by the Austrian Science Fund (FWF) Project P29731-N36.

Data availability statement

All data that support the findings of this study are included within the article (and any supplementary files).

ORCID iDs

Dominik Legut https://orcid.org/0000-0001-9185-9934
Claudia Draxl https://orcid.org/0000-0003-3523-6657

References

[1] Appel F and Wagner R 1998 *Mater. Sci. Eng.* R **22** 187
[2] Wallgram W, Schmölzer T, Cha L, Das G, Güther V and Clemens H 2009 *Int. J. Mater. Res.* **100** 8
[3] Ye H Q 1999 *Mater. Sci. Eng.* A **263** 289
[4] Herrouin F, Hu D, Bowen P and Jones I P 1998 *Acta Mater.* **46** 4963
[5] Westbrook J H 1994 *Intermetallic Compounds-Principles and Practice* ed J H Westbrook and R L Fleischer vol 1 (New York: Wiley)
[6] Gao Y, Zhu J, Shen H and Wang Y 1993 *Scr. Metall. Mater.* **28** 651
[7] Benedek R, van de Walle A, Gerstl S S A, Asta M and Seidman D N 2005 *Phys. Rev.* B **71** 094201
[8] Music D and Schneider J M 2006 *Phys. Rev.* B **74** 174110
[9] Fu H, Li D, Peng F, Gao T and Cheng X 2009 *J. Alloys Compd.* **473** 255
[10] Li H, Wang S and Ye H 2009 *J. Mater. Sci. Technol.* **25** 569-76
[11] Liu S, Shang J, Wang F and Zhang Y 2009 *Phys. Rev.* B **79** 075419
[12] Izumi T, Nishimoto T and Narita T 2003 *Intermetallics* **11** 841
[13] Song Y, Guo Z X, Yang R and Li D 2002 *Comput. Mater. Sci.* **23** 55
[14] Liu Y L, Liu L M, Wang S Q and Ye H Q 2007 *Intermetallics* **15** 428
[15] Zhou H-B, Zhang Y, Liu Y-L, Kohyama M, Yin P-G and Lu G-H 2009 *J. Phys.: Condens. Matter* **21** 175407
[16] Denquin A, Naka S, Huguet A and Menand A 1993 *Scr. Metall. Mater.* **28** 1131
[17] Huguet A and Menand A 1994 *Appl. Surf. Sci.* **76–77** 191
[18] Menand A, Huguet A and Nérac-Partaix A 1996 *Acta Mater.* **44** 4729
[19] Kawabata T, Tadano M and Izumi O 1991 *ISIJ Int.* **31** 1161
[20] Perdrix F, Trichet M-F, Bonnentien J-L, Cornet M and Bigot J 2001 *Intermetallics* **9** 807
[21] Jeitschko W, Nowotny H and Benesovsky F 1964 *J. Less-Common Met.* **7** 133
[22] Matar S F and Etourneau J 1996 *J. Alloys Compd.* **233** 112
[23] Lu Z W, Zunger A and Fox A G 1994 *Acta Metall. Mater.* **42** 3929
[24] Kanchana V 2009 *Europhys. Lett.* **87** 26006
[25] Matar S F, Petitcorps Y L and Etourneau J 1997 *J. Mater. Chem.* **7** 99
[26] Hug G, Jaouen M and Barsoum M W 2005 *Phys. Rev.* B **71** 024105
[27] Willhelmsson O *et al* 2006 *J. Cryst. Growth* **291** 290
[28] Kresse G and Furthmüller J 1996 *Phys. Rev.* B **54** 11169
[29] Perdew J P, Burke K and Ernzerhof M 1996 *Phys. Rev. Lett.* **77** 3865
[30] Methfessel M and Paxton A T 1989 *Phys. Rev.* B **40** 3616
[31] Scheu C, Stergar E, Schober M, Cha L, Clemens H, Bartels A, Schimansky F-P and Cerezo A 2009 *Acta Mater.* **57** 1504
[32] Pearson W B 1967 *Handbook of Lattice Spacings and Structures of Metals and Alloys* (Oxford: Pergamon)
[33] He Y, Schwarz R B, Migliori A and Whang S H 1995 *J. Mater. Res.* **10** 1187
[34] Tanaka K, Ichitsubu T, Iniu H, Yamaguchi M and Koiwa M 1996 *Phil. Mag. Lett.* **73** 71

[35] Fu L and Yoo M 1991 *Alloy Phase Stablity and Design* ed G M Stocks, D P Pope and A F Giamei (Pittsburgh: Materials Research Society)
[36] Mehl M J, Klein B M and Papaconstatopoulos D A 1994 *Intermetallic Compounds: Principles and Applications* ed J H Westbrook and R L Fleischer (New York: Wiley)
[37] Woodward C, Kajihara S and Yang L H 1998 *Phys. Rev.* B **57** 13459
[38] Tanaka K, Okamoto K, Inui H, Minonishi Y, Yamaguchi M and Koiwa M 1996 *Phil. Mag.* A **73** 1475
[39] Yu R, Zhu J and Ye H Q 2010 *Comput. Phys. Commun.* **181** 671
[40] Tanaka K and Koiwa M 1996 *Intermetallics* **4** S29
[41] Birch F 1947 *Phys. Rev.* **71** 809
[42] Siegl R, Vitek V, Inui H, Kishida K and Yamaguchi M 1997 *Phil. Mag.* A **75** 1447
[43] Solozhenko V L and Kurakevych O O 2005 *Solid State Commun.* **133** 385
[44] Ramqvist LHamrin KJohansson GGelius UNordling C 1968 VC, NbC and TaC with varying carbon content studied by ESCA *J. Ann.* **517** 2669-72
[45] Tian W H and Nemoto M 1997 *Intermetallics* **5** 237
[46] Gesing T.M.Jeitschko W. 1995 The Crystal Structure and Chemical Properties of U2Al3C4 and Structure Refinement of Al4C3 *Z. Naturforsch. b* **50** 196-200
[47] Zhang R F, Argon A S and Veprek S 2009 *Phys. Rev. Lett.* **102** 015503
[48] Alouani M, Albers R C and Methfessel M 1991 *Phys. Rev.* B **43** 6500
[49] Beckstein O, Klepeis J E, Hart G L W and Pankratov O 2001 *Phys. Rev.* B **63** 134112
[50] Nye J F 1957 *Physical Properties of Crystals: Their Representation by Tensors and Matrices* (Oxford: Oxford Press)
[51] Wallace D C 1972 *Thermodynamics of Crystals* (New York: Wiley)
[52] Grimvall G 1999 *Thermophysical Properties of Materials* (Amsterdam: North-Holland)
[53] Van de Walle C G, Laks D B, Neumark G F and Pantelides S T 1993 *Phys. Rev.* B **47** 9425
[54] Van de Walle C G and Neugebauer J 2004 *J. Appl. Phys.* **95** 3851
[55] Fu C L and Yoo M H 1990 *Phil. Mag. Lett.* **62** 159
[56] Nguyen-Manh D, Vitek V and Horsfield A 2007 *Prog. Mater. Sci.* **52** 255
[57] The shear directions and planes in reference [57], p 160, for the C_{44} and C_{66} are interchanged. In fact, C_{44} corresponds to a [100] shear in the (010) plane and C_{66} to a [010] shear in the (001) plane.
[58] Pettifor D G 1991 *Phil. Trans. R. Soc.* A **334** 439
[59] Pugh S F 1954 *London, Edinburgh Dublin Phil. Mag. J. Sci.* **45** 823
[60] Hill R 1952 *Proc. Phys. Soc.* A **65** 349
[61] Hashin Z and Shtrikman S 1962 *J. Mech. Phys. Solids* **10** 343
[62] Chu F, Mitchell T E, Majumdar B, Miracle D, Nandy T K and Banerjee D 1997 *Intermetallics* **5** 147
[63] Ledbetter H M 1973 *J. Appl. Phys.* **44** 1451
[64] Chen S, Beaven P A and Wagner R 1992 *Scr. Metall. Mater.* **26** 1205
[65] Mishin Y and Herzig C 2000 *Acta Mater.* **48** 589
[66] A 32 atom supercell of γ-TiAl with C on Al-site has a c/a ratio of 1, as seen from figure 8. However, the atoms surrounding C relax into a lower symmetry, hence the stability conditions for tetragonal systems are valid.
[67] Qing-Gong S, Guo-Shun Q, Bao-Bao Y, Qing-Jie J and Xue-Lan H 2016 *Acta Phys. Sin.* **65** 046102
[68] Hai-Yan W, Qian-Ku H, Wen-Peng Y and Xu-Sheng L 2016 *Acta Phys. Sin.* **65** 077101
[69] Saeedipour S, Kermanpur A and Sadeghi F 2020 *J. Alloys Compd.* **817** 152749
[70] Liu Y, Chen K, Zhang J, Hu Z, Lu G and Kioussis N 1997 *J. Phys.: Condens. Matter* **9** 9829
[71] Tian W H and Nemoto M 1997 *Intermetallics* **5** 237
[72] Appel F, Oehring M and Wagner R 2000 *Intermetallics* **8** 1283
[73] Wang Q, Ding H, Zhang H, Chen R, Guo J and Fu H 2017 *Mater. Sci. Eng.* A **700** 198
[74] Holec D, Reddy R K, Klein T and Clemens H 2016 *J. Appl. Phys.* **119** 205104
[75] Jacob K T, Raj S and Rannesh L 2007 *Ing. J. Mater. Res.* **98** 9
[76] Hom T, Kiszenik W and Post B 1975 *J. Appl. Cryst.* **8** 457
[77] Trucano P, Chen R, Gamlen P H and White J W 1975 *Nature* **258** 136
[78] Kokalj A 1999 *J. Mol. Graphics Modell.* **17** 176–9
[79] The errors of our calculations are indeed smaller, but we investigate defect-free materials, hence C_{ij}, Si, and Ai can deviate from their experimental counterparts.